Editors' Suggestion

Relativistic effects in the multiphoton ionization of hydrogenlike ions by ultrashort infrared laser pulses

Charles J. Joachain and Niels J. Kylstra*

Physique Théorique et Mathématique, C.P. 227, Université Libre de Bruxelles, B-1050 Brussels, Belgium

(Received 17 March 2019; published 23 July 2019)

The direct multiphoton ionization (MPI) of hydrogenlike ions by intense, linearly polarized, ultrashort infrared laser pulses is investigated within the framework of the strong field approximation (SFA) for laser peak intensities and angular frequencies where relativistic effects are important. We obtain an expression for the differential MPI probability using the Dirac equation and demonstrate that, for the particular case of light ions, the Dirac spin-unresolved MPI probabilities agree with those obtained using the Klein-Gordon equation as well as the relativistic Schrödinger equation. As an example, the interaction of hydrogenlike neon ions with an intense four-cycle Ti:sapphire laser pulse is considered. We show that, in contrast to the nonrelativistic regime, for ultrashort pulses in the relativistic regime, interference effects do not play a role in determining the main features of the energy-resolved photoelectron spectrum. Moreover, we find that the angle-integrated photoelectron spectrum can be obtained using the well-known nonrelativistic SFA formula, properly adjusted to account for the electron drift along the laser propagation direction.

DOI: 10.1103/PhysRevA.100.013417

I. INTRODUCTION

Table-top infrared lasers systems have been developed that are capable of producing short pulses with peak intensities exceeding 10^{22} W/cm^2 [1,2]. The interaction of atomic systems with pulses produced by these lasers must be described by a relativistic theory, as in this frequency and intensity regime the quiver, or ponderomotive, energy of an electron in the pulse is larger than its rest mass energy. In this paper we will investigate, using the strong field approximation (SFA) [3–5], the direct (i.e., without recollisions) multiphoton ionization (MPI) of hydrogenlike ions interacting with intense, linearly polarized, ultrashort, infrared laser pulses.

At lower laser peak intensities, where a nonrelativistic description is appropriate, the SFA has proved to be a successful approach for describing the interaction of atomic systems with laser pulses in the low frequency regime where the Keldysh parameter is small [6,7]. Moreover, it provides a simple quasiclassical interpretation of the MPI process [8]. In addition to applications to direct MPI, the SFA has also been used to investigate high harmonic generation [9,10], recollision effects [11], and double ionization processes [12] in intense laser fields. Coulomb corrections, which are necessary for describing features of the low-energy ejected electron spectrum, have also been incorporated within the framework of the SFA [13–16].

The extension of the SFA to the relativistic regime has been considered by Reiss [17], and has been used in recent studies of relativistic MPI [18–20]. For laser pulses having very low frequencies, an adiabatic approximation can be made, and the total MPI probability can be calculated using tunneling formulas [21–23]. Coulomb corrections [24], spin effects [25,26], as well as MPI by ultrashort pulses [27] have also been investigated.

We would also like to mention recent studies in which the Dirac equation has been solved numerically to obtain ionization probabilities. In particular, Bauke *et al.* [28] considered the ionization of highly charged hydrogenlike ions in short intense laser pulses as a function of the laser pulse parameters. Investigations have also been carried out in higher frequency regimes [29–32].

In the following section we state the basic results that will be needed to obtain the Dirac direct ionization amplitude in the SFA. We then give the SFA direct MPI amplitude, evaluate it using the saddle point method. and obtain the spin-unresolved ionization probability. In the subsequent two sections, we derive the SFA MPI amplitudes using the Klein-Gordon and relativistic Schrödinger equations, respectively. As an example, the theory is then applied to the ionization of hydrogenlike neon by an ultrashort, intense Ti:sapphire laser pulse. We conclude by summarizing our findings.

II. THE DIRAC EQUATION

Our starting point is the Dirac equation in S.I. units describing an electron of mass m and charge $-e$ in an electromagnetic field:

$$i\hbar\frac{\partial}{\partial t}\Psi(\boldsymbol{r},t) = H^{\rm D}\,\Psi(\boldsymbol{r},t), \tag{1}$$

where the Dirac Hamiltonian is

$$\begin{aligned} H^{\rm D} &= H_0^{\rm D} + H_{\rm Int}^{\rm D} + V \\ &= c\boldsymbol{\alpha}\cdot(-i\hbar\nabla + e\boldsymbol{A}) + \beta mc^2 + V, \end{aligned} \tag{2}$$

with $H_0^{\rm D} = c\boldsymbol{\alpha}\cdot(-i\hbar\nabla) + \beta mc^2$ and $H_{\rm Int}^{\rm D} = ce\boldsymbol{\alpha}\cdot\boldsymbol{A}$. Here c is the speed of light, $\boldsymbol{\alpha} = (\alpha_x, \alpha_y, \alpha_z)$ and β are 4×4

*niels.kylstra@gmail.com

matrices that, in the Dirac representation, are given by

$$\boldsymbol{\alpha} = \begin{pmatrix} 0 & \boldsymbol{\sigma} \\ \boldsymbol{\sigma} & 0 \end{pmatrix}, \qquad \beta = \begin{pmatrix} I & 0 \\ 0 & -I \end{pmatrix}. \tag{3}$$

The Pauli matrices are defined as

$$\sigma_x = \begin{pmatrix} 0 & 1 \\ 1 & 0 \end{pmatrix}, \quad \sigma_y = \begin{pmatrix} 0 & -i \\ i & 0 \end{pmatrix}, \quad \sigma_z = \begin{pmatrix} 1 & 0 \\ 0 & -1 \end{pmatrix}. \tag{4}$$

The electron interacts via the Coulomb potential with a nucleus having atomic number Z, so that

$$V(r) = -\frac{e^2 Z}{(4\pi\epsilon_0)r} = -\frac{c\alpha\hbar Z}{r}, \tag{5}$$

where α is the fine structure constant. The laser pulse is described by the vector potential

$$\boldsymbol{A}(\eta) = \hat{\boldsymbol{\epsilon}} A_0 \cos(\eta + \varphi)\zeta(\eta), \tag{6}$$

with $\eta = \omega t - \boldsymbol{k}_{\rm L} \cdot \boldsymbol{r}$ and $\boldsymbol{k}_{\rm L} = \hat{\boldsymbol{k}}_{\rm L}\omega/c$, where ω is the carrier angular frequency. Here $\zeta(\cdot)$ is the laser pulse envelope function and φ is the carrier-envelope phase. The laser propagation direction is along $\hat{\boldsymbol{k}}_{\rm L}$ (which is perpendicular to $\hat{\boldsymbol{\epsilon}}$) and $\mathcal{E}_0 = \omega A_0$ is the peak electric field strength of the laser field. Hereby a constant wave-front approximation is made, which is applicable when the laser pulse is not tightly focused.

In the absence of the laser field, the unperturbed Dirac Hamiltonian describing the hydrogenlike ion is $H_0^{\rm D} + V$. The eigenstates of this Hamiltonian are known, and the wave function of the ground state of the system can be expressed as [33]

$$\phi_{0s}(\boldsymbol{r}, t) = v_{0s}(\hat{\boldsymbol{r}})\psi_0^{\rm D}(r)\exp[i(I_{\rm p} - mc^2)t/\hbar] \tag{7}$$

with

$$\psi_0^{\rm D}(r) = \left(\frac{\kappa^3(2-\gamma)}{\pi\Gamma(3-2\gamma)}\right)^{1/2}(2\kappa r)^{-\gamma}\exp(-\kappa r) \tag{8}$$

and

$$v_{0s}(\hat{\boldsymbol{r}}) = \begin{pmatrix} \chi^s \\ i\boldsymbol{\sigma}\cdot\tilde{\boldsymbol{r}}\chi^s \end{pmatrix}. \tag{9}$$

Here $\gamma = I_{\rm p}/(mc^2)$, $I_{\rm p} = mc^2 - (m^2c^4 - c^2\hbar^2\kappa^2)^{1/2}$, $\hbar\kappa = mcZ\alpha$, and $\Gamma(\cdot)$ is the Euler gamma function. In addition, we have introduced the vector $\tilde{\boldsymbol{r}} = I_{\rm p}\hat{\boldsymbol{r}}/(c\kappa)$ as well as the spinors $\chi^{\uparrow} = \binom{1}{0}$ and $\chi^{\downarrow} = \binom{0}{1}$ corresponding to the spin-up ($s =\uparrow$) and spin-down ($s =\downarrow$) electron states, respectively.

The Dirac-Volkov (DV) wave function [34], which is a solution of Eq. (1) with $V = 0$ in $H^{\rm D}$, is given by

$$\chi_{\boldsymbol{p}s}^{\rm DV}(\boldsymbol{r}, t) = J(\eta)u_{\boldsymbol{p}s}\chi_{\boldsymbol{p}}(\boldsymbol{r}, t) \tag{10}$$

with the plane-wave positive energy four-component spinor $u_{\boldsymbol{p}s}$ being

$$u_{\boldsymbol{p}s} = N^{1/2}\begin{pmatrix} \chi^s \\ \boldsymbol{\sigma}\cdot\tilde{\boldsymbol{p}}\chi^s \end{pmatrix}, \tag{11}$$

and the normalization factor, $N = (E_p + mc^2)/(2E_p)$, has been chosen such that the plane-wave density is constant. We have also made use of the dimensionless quantity $\tilde{\boldsymbol{p}} = c\boldsymbol{p}/(E_p + mc^2)$. The Klein-Gordon-Volkov (KGV) laser-dressed plane waves are

$$\chi_{\boldsymbol{p}}(\boldsymbol{r}, t) = (2\pi\hbar)^{-3/2}\exp[i(\boldsymbol{p}\cdot\boldsymbol{r} - E_p t)/\hbar]g(\eta) \tag{12}$$

with momentum $\boldsymbol{p}$ having components (p_E, p_B, p_k) along the laser electric field, magnetic field, and propagation directions, respectively, and energy

$$E_p = (m^2c^4 + c^2\boldsymbol{p}^2)^{1/2}. \tag{13}$$

The function $g(\eta)$ appearing in Eq. (12) satisfies the ordinary differential equation

$$i\frac{d}{d\eta}g(\eta) = \beta(\eta)g(\eta). \tag{14}$$

The quantity

$$\beta(\eta) = \frac{1}{2\hbar\omega m\Lambda}[2e\boldsymbol{p}\cdot\boldsymbol{A}(\eta) + e^2A^2(\eta)] \tag{15}$$

is dimensionless, as is

$$\Lambda = \frac{E_p - cp_k}{mc^2}, \tag{16}$$

which is a constant of the motion. The initial condition $g(\eta \to -\infty) = 1$ must be satisfied, hence the required solution of Eq. (14) is

$$g(\eta) = \exp\left(-i\int_{-\infty}^{\eta} d\eta' \beta(\eta')\right). \tag{17}$$

Finally, the matrix $J(\eta)$ in Eq. (10) is defined as

$$J(\eta) = I + (I + \boldsymbol{\alpha}\cdot\hat{\boldsymbol{k}}_{\rm L})\boldsymbol{\alpha}\cdot\tilde{\boldsymbol{A}}(\eta), \tag{18}$$

where I is the unit matrix and $\tilde{\boldsymbol{A}}(\eta) = e\boldsymbol{A}(\eta)/(2mc\Lambda)$.

In what follows, we will work in the Göppert-Mayer gauge, obtained by applying the unitary transformation

$$\Psi' = \exp[ie\boldsymbol{r}\cdot\boldsymbol{A}(\eta)/\hbar]\Psi. \tag{19}$$

The resulting Hamiltonian, which now depends on the electric field component of the laser pulse, $\boldsymbol{\mathcal{E}} = -\partial\boldsymbol{A}/\partial t$, is

$$H^{\rm D} = c\boldsymbol{\alpha}\cdot\left[-i\hbar\nabla - \frac{e}{c}(\boldsymbol{r}\cdot\boldsymbol{\mathcal{E}})\hat{\boldsymbol{k}}_{\rm L}\right] + \beta mc^2 + e\boldsymbol{r}\cdot\boldsymbol{\mathcal{E}} + V, \tag{20}$$

and the KGV wave function becomes

$$\chi_{\boldsymbol{p}}(\boldsymbol{r}, t) = (2\pi\hbar)^{-3/2}\exp[i(\boldsymbol{p}\cdot\boldsymbol{r} - E_p t)/\hbar]g(\boldsymbol{r}, \eta), \tag{21}$$

with $g(\boldsymbol{r}, \eta) = \exp[ie\boldsymbol{r}\cdot\boldsymbol{A}(\eta)/\hbar]g(\eta)$.

III. THE SFA DIRECT MULTIPHOTON IONIZATION PROBABILITY

The SFA direct MPI amplitude is given by

$$T_{\boldsymbol{p}s',0s}^{\rm SFA} = \frac{1}{i\hbar}\int_{-\infty}^{\infty} dt\langle\chi_{\boldsymbol{p}s'}^{\rm DV}(t)\big|H_{\rm Int}^{\rm D}(t)|\phi_{0s}(t)\rangle. \tag{22}$$

It is convenient to write

$$H_{\rm Int}^{\rm D}(t) = \left[H_0^{\rm D} + H_{\rm Int}^{\rm D}(t)\right] - \left(H_0^{\rm D} + V\right) + V, \tag{23}$$

and then to perform the integration in Equation (22) by parts, which yields

$$T_{\boldsymbol{p}s',0s}^{\rm SFA} = \frac{1}{i\hbar}\int_{-\infty}^{\infty} dt \langle \chi_{\boldsymbol{p}s'}^{\rm DV}(t)|V|\phi_{0s}(t)\rangle. \tag{24}$$

The spin-unresolved probability density that the unpolarized atom or ion will eject an electron having a kinetic energy $E = E_p - mc^2$ within the interval $(E, E+dE)$ and into the solid angle $d\hat{\boldsymbol{p}}$ centered about $\hat{\boldsymbol{p}}$ is then given by

$$dP^{\rm SFA}(E,\hat{\boldsymbol{p}}) = \frac{1}{2}\left[\frac{E(E+mc^2)^2(E+2mc^2)}{c^6}\right]^{1/2} \times \sum_{s,s'=\uparrow,\downarrow} \left|T_{\boldsymbol{p}s',0s}^{\rm SFA}\right|^2 dE\, d\hat{\boldsymbol{p}}. \tag{25}$$

Returning to the transition amplitude Eq. (24) and making use of Eq. (21), allows us to write

$$\begin{aligned} T_{\boldsymbol{p}s',0s}^{\rm SFA} &= \frac{1}{i(2\pi)^{3/2}\hbar^{5/2}}\int_{-\infty}^{\infty} dt \int d\boldsymbol{r}\, M_{\boldsymbol{p}}^{s's}(\eta,\hat{\boldsymbol{r}}) \\ &\quad \times \exp(-i[\boldsymbol{p}\cdot\boldsymbol{r} - (E+I_{\rm p})t]/\hbar) g^*(\boldsymbol{r},\eta)V(r)\psi_0^{\rm D}(\boldsymbol{r}) \\ &= \frac{1}{i\hbar}\int_{-\infty}^{\infty} dt \langle \boldsymbol{\pi}(t)|M_{\boldsymbol{p}}^{s's}(\omega t)V|\psi_0^{\rm D}\rangle \exp[iS(t)]. \end{aligned} \tag{26}$$

In this expression, we have introduced the spin transition amplitude

$$M_{\boldsymbol{p}}^{s's}(\eta,\hat{\boldsymbol{r}}) = u_{\boldsymbol{p}s'}^{\dagger} J^{\dagger}(\eta) v_{0s}(\hat{\boldsymbol{r}}) \tag{27}$$

and have defined the shifted momentum $\boldsymbol{\pi}(t) = \boldsymbol{p} - q\hbar\boldsymbol{k}_{\rm L} + e\boldsymbol{A}(\omega t)$, with $q = (E+I_{\rm p})/(\hbar\omega)$. In Equation (26), the quasiclassical action is

$$S(t) = q\omega t + \omega\int_{-\infty}^{t} dt'\beta(\omega t'). \tag{28}$$

It will be convenient to work instead with the quantity

$$\tilde{S}(t) = q\omega t - \omega\int_{t}^{\infty} dt'\beta(\omega t'), \tag{29}$$

which introduces an immaterial phase factor to the transition amplitude.

The spin transition amplitude $M_{\boldsymbol{p}}^{s's}(\eta,\hat{\boldsymbol{r}})$ consists of two contributions. The first couples the large components of the initial and final state spinors, respectively, and is given by

$$M_{{\rm L},\boldsymbol{p}}^{s's}(\eta) = N^{1/2}\chi^{s'}[(1+\tilde{\boldsymbol{p}}\cdot\tilde{\boldsymbol{A}})I - i\boldsymbol{\sigma}\cdot(\boldsymbol{k}_{\rm L} - \tilde{\boldsymbol{p}})\times\tilde{\boldsymbol{A}}]\chi^{s}, \tag{30}$$

while the second term,

$$M_{{\rm S},\boldsymbol{p}}^{s's}(\eta,\hat{\boldsymbol{r}}) = N^{1/2}\chi^{s'}[(\boldsymbol{k}_{\rm L}\times\tilde{\boldsymbol{A}})\cdot\tilde{\boldsymbol{p}}I + i\boldsymbol{\sigma} \cdot(\tilde{\boldsymbol{p}} + \tilde{\boldsymbol{A}} - (\boldsymbol{k}_{\rm L}\times\tilde{\boldsymbol{A}})\times\tilde{\boldsymbol{p}})]\boldsymbol{\sigma}\cdot\tilde{\boldsymbol{r}}\chi^{s}, \tag{31}$$

couples the corresponding small components.

When evaluating Eq. (26), the following atomic transition matrix elements appear:

$$\langle\boldsymbol{p}|V|\psi_0^{\rm D}\rangle = \frac{1}{k}C_\gamma f(-\gamma,\kappa,k) \tag{32}$$

and

$$\langle\boldsymbol{p}|\hat{\boldsymbol{r}}V|\psi_0^{\rm D}\rangle = \frac{i\hat{\boldsymbol{k}}}{k}C_\gamma\left[\frac{1}{k}f(-1-\gamma,\kappa,k) - \frac{d}{dk}f(-1-\gamma,\kappa,k)\right]. \tag{33}$$

In these expressions, $\boldsymbol{k} = k\hat{\boldsymbol{k}} = \boldsymbol{p}/\hbar$, and we have introduced the quantity

$$C_\gamma = -\frac{cZ\alpha(2\kappa)^{-\gamma}}{2\pi}\left(\frac{(2\kappa)^3(2-\gamma)}{\hbar\Gamma(3-2\gamma)}\right)^{1/2} \tag{34}$$

as well as the function

$$\begin{aligned} f(a,\kappa,k) &= \int_0^\infty dr\, r^a \exp(-\kappa r)\sin(kr) \\ &= \frac{\Gamma(1+a)\sin[(1+a)\arctan(k/\kappa)]}{(\kappa^2+k^2)^{(1+a)/2}} \end{aligned} \tag{35}$$

for $a > -2$.

The integration over time in Eq. (26) can be carried out numerically. However, we will follow the usual procedure and obtain an approximation based on the saddle point method [35]. The complex saddle times, t_s, are determined by the condition $d\tilde{S}(t)/dt = 0$, or

$$q\hbar\omega + \frac{1}{2m\Lambda}[2e\boldsymbol{p}\cdot\boldsymbol{A}(\omega t_s) + e^2A^2(\omega t_s)] = 0, \tag{36}$$

which leads to

$$eA(\omega t_s) = -p_E \pm \sqrt{p_E^2 - 2qm\hbar\omega\Lambda}. \tag{37}$$

We note that this equation may also be written as

$$\begin{aligned} eA(\omega t_s) &= -p_E \pm i\sqrt{(E/c - p_k)^2 + p_B^2 + 2mI_{\rm p}\Lambda} \\ &= -p_E \pm i\sqrt{m^2c^2(\Lambda-1)^2 + p_B^2 + 2mI_{\rm p}\Lambda}. \end{aligned} \tag{38}$$

Equation (37) or (38) can be readily solved numerically to obtain the saddle times.

Considering now the limit $I_{\rm p}\to 0$, we see that the saddle times correspond to the classical detachment times in the laser field. Hence t_s is real, with $p_E = \pm(2mE)^{1/2}$, $p_k = E/c = p_E^2/(2mc)$, $p_B = 0$, and $\Lambda = 1$. This provides the motivation to make the approximation

$$t_s \simeq t_d + it_c, \tag{39}$$

where t_d is the classical detachment time and t_c is assumed to be small. The imaginary part of the saddle time gives rise to a complex quasiclassical action, the imaginary part of which can be identified as a tunneling ionization amplitude. To calculate the segment of the time integral from it_c to t_d, we use the fact that $eA(\omega t_d) \simeq -p_E$, and obtain

$${\rm Im}\tilde{S}(t_s) \simeq \frac{1}{3m\Lambda}\frac{\left[2m(E+I_{\rm p})\Lambda - p_E^2\right]^{3/2}}{|e\boldsymbol{\mathcal{E}}(\omega t_d)|}. \tag{40}$$

When $\gamma = I_{\rm p}/(mc^2) \ll 1$ and for fixed p_E, the quantity ${\rm Im}\tilde{S}(t_s)$ is minimized when $p_k \simeq p_k^{\rm m} = \gamma mc/3 + p_E^2/(2mc)(1+\gamma/3)$, so that electron emission is most probable along a parabola in the p_E-p_k plane.

Let us now return to Eq. (31). This quantity is zero when evaluated at the classical detachment time t_d, and is of order γ smaller than the amplitude given by Eq. (30) when evaluated at the complex saddle time t_s and with p_k given by its most probable value. When considering light hydrogenlike ions, as we do here, the contribution to the SFA direct ionization of the small components of the initial (and final) wave function can therefore be safely neglected.

We now point out that the atomic transition matrix element of Eq. (32) is singular at the saddle time, as in the limit $t \to t_s$ we have that $\boldsymbol{\pi}^2(t_s) = -\hbar^2\kappa^2$. Here we focus on ions with $\gamma \ll 1$, hence the evaluation of the transition amplitude (26) at the saddle time can be performed by setting $\gamma = 0$. Expanding the denominator in the resulting approximation for Eq. (32) in powers of $(t - t_s)$, and assuming that there is no confluence of saddle times, results in the following expression for the amplitude:

$$T^{\text{SFA}}_{\boldsymbol{p}s',0s} = -\frac{c\alpha Z(2\kappa)^{3/2}}{4m(\hbar)^{1/2}\Lambda}\sum_{t_s} M^{s's}_{\text{L},\boldsymbol{p}}(\omega t_s)\frac{\exp[i\tilde{S}(t_s)]}{\tilde{S}''(t_s)}. \tag{41}$$

The procedure used to obtain Eq. (40) gives

$$\tilde{S}''(t_s) \simeq \frac{i|e\boldsymbol{\mathcal{E}}(\omega t_d)|}{m\hbar\Lambda}\left[2m(E + I_\text{p})\Lambda - p_E^2\right]^{1/2} \tag{42}$$

for the second derivative of the quasiclassical action at the saddle time. Choosing the quantization axis to be along the laser magnetic field direction and making use of Eq. (38), the components of the spin transition amplitudes of Eq. (30) can be expressed as

$$\begin{aligned} M^{++}_{\text{L},\boldsymbol{p}}(\omega t_s) = M^{--}_{\text{L},\boldsymbol{p}}(\omega t_s) &\simeq \frac{N^{1/2}}{1 + (\epsilon/2)} \\ &\times \left\{1 + \left(\frac{\epsilon\gamma}{4}\right)^{1/2} + i\left[\left(\frac{\epsilon}{2}\right)^{1/2} - \left(\frac{\gamma}{2}\right)^{1/2}\right]\right\}, \\ M^{+-}_{\text{L},\boldsymbol{p}}(\omega t_s) = M^{-+}_{\text{L},\boldsymbol{p}}(\omega t_s) &= 0, \end{aligned} \tag{43}$$

where we have set p_k and p_B to their most likely values. In addition, we have introduced the quantity $\epsilon = E/(mc^2)$ and have only included the terms of lowest order in powers of γ. Then,

$$\begin{aligned} \frac{1}{2}\sum_{s,s'=\uparrow,\downarrow}\left|T^{\text{SFA}}_{\boldsymbol{p}s',0s}\right|^2 &= \frac{1}{2}\left|T^{\text{SFA}}_{\boldsymbol{p},0}\right|^2\sum_{s,s'=\uparrow,\downarrow}\left|M^{s's}_{\text{L},\boldsymbol{p}}(\omega t_s)\right|^2 \\ &= \frac{1 + (\gamma/2)}{1 + \epsilon}\left|T^{\text{SFA}}_{\boldsymbol{p},0}\right|^2 \simeq \frac{mc^2}{E + mc^2}\left|T^{\text{SFA}}_{\boldsymbol{p},0}\right|^2 \end{aligned} \tag{44}$$

where the spin-independent SFA transition amplitude

$$T^{\text{SFA}}_{\boldsymbol{p},0} = \sum_{t_s} a_{\text{ion}}(t_s)a_{\text{field}}(t_s) \tag{45}$$

is expressed in terms of two amplitudes. The first is the ionization amplitude

$$\begin{aligned} a_{\text{ion}}(t_s) = &\frac{ic\alpha Z(2\hbar\kappa)^{3/2}}{4\hbar|e\boldsymbol{\mathcal{E}}(\omega t_d)|\left[2m(E + I_\text{p})\Lambda - p_E^2\right]^{1/2}} \\ &\times \exp\left(-\frac{\left[2m(E + I_\text{p})\Lambda - p_E^2\right]^{3/2}}{3m\Lambda|e\boldsymbol{\mathcal{E}}(\omega t_d)|}\right) \end{aligned} \tag{46}$$

that depends on the magnitude of electric field component of the laser pulse at the classical detachment times. The second is associated with the evolution of the ejected electron in the laser field,

$$a_{\text{field}}(t_s) = \exp[i\tilde{S}(t_d)]. \tag{47}$$

Making use of Eq. (44) the spin-unresolved SFA direct MPI probability density, Eq. (25), becomes

$$dP^{\text{SFA}}(E, \hat{\boldsymbol{p}}) = \left[\frac{m^2E(E + 2mc^2)}{c^2}\right]^{1/2}\left|T^{\text{SFA}}_{\boldsymbol{p},0}\right|^2 dE\, d\hat{\boldsymbol{p}}. \tag{48}$$

This expression is of exactly the same form as in the nonrelativistic SFA. Indeed the well-known SFA result is obtained by setting $\Lambda = 1$ in Eq. (46) and in Eq. (15) when evaluating $\tilde{S}(t_d)$. Of course in this nonrelativistic limit $\hbar\kappa = (2mI_\text{p})^{1/2}$, $I_\text{p} = mc^2Z^2\alpha^2/2$, and $E = \boldsymbol{p}^2/(2m)$. We will return to the relationship between the relativistic and nonrelativistic SFA MPI probabilities below.

IV. KLEIN-GORDON SFA

As we only consider the spin-unresolved MPI probabilities, it is of interest to neglect from the onset the spin degrees of freedom of the atomic system. In this section we compare the Dirac-SFA direct MPI probability obtained above with the corresponding result obtained within the framework of the Klein-Gordon equation. Making use of the two-component formalism of Feshbach and Villars [36], the Klein-Gordon equation in the Hamiltonian form is expressed as

$$i\hbar\frac{\partial}{\partial t}\bar{\Psi}(\boldsymbol{r}, t) = H^{\text{KG}}\bar{\Psi}(\boldsymbol{r}, t), \tag{49}$$

where $H^{\text{KG}} = H_0^{\text{KG}} + H_{\text{Int}}^{\text{KG}} + V$ is a matrix operator with

$$H^{\text{KG}} = \frac{1}{2m}(-i\hbar\boldsymbol{\nabla} + e\boldsymbol{A})^2(i\sigma_y + \sigma_z) + mc^2\sigma_z + V, \tag{50}$$

$$H_0^{\text{KG}} = \frac{1}{2m}(-i\hbar\boldsymbol{\nabla})^2(i\sigma_y + \sigma_z) + mc^2\sigma_z. \tag{51}$$

The wave function $\bar{\Psi}(\boldsymbol{r}, t)$ has two charge components, which we label by "−" and "+", respectively.

It is readily verified that for the initial state of the system these components are given by

$$\begin{aligned} \phi_0^{\mp}(\boldsymbol{r}, t) = &\frac{1}{2}\left(\frac{1}{1 + \gamma}\right)^{1/2}\left(1 \pm \left[1 - \gamma - \frac{V(r)}{mc^2}\right]\right) \\ &\times \psi_0(\boldsymbol{r})\exp[i(I_\text{p} - mc^2)t/\hbar], \end{aligned} \tag{52}$$

where for the particular case of a hydrogenlike ion in its ground state the ionization potential is [37]

$$I_\text{p} = mc^2 - mc^2[1 + 4Z^2\alpha^2/(1 + \sigma)^2]^{-1/2} \tag{53}$$

and the time-independent wave function $\psi_0(\boldsymbol{r})$, which is the ground state solution of the second-order Klein-Gordon equation, is

$$\psi_0(\boldsymbol{r}) = \left[\frac{(2\kappa)^3}{4\pi\Gamma(\sigma + 2)}\right]^{1/2}(2\kappa r)^{(\sigma-1)/2}\exp(-\kappa r). \tag{54}$$

Here $\sigma = (1 - 4Z^2\alpha^2)^{1/2}$ and $\hbar\kappa = (2mI_\text{p} - I_\text{p}^2/c^2)^{1/2}$.

For the case in which the electron is interacting with the laser field and $V = 0$, one finds that the wave function components can be expressed in terms of the KGV wave function of Eq. (12) as

$$\chi_{\boldsymbol{p}}^{\mp}(\boldsymbol{r}, t) = \frac{[mc^2 \pm \{E_p + \hbar\omega\beta(\eta)\}]}{2(mc^2 E_p)^{1/2}} \chi_{\boldsymbol{p}}(\boldsymbol{r}, t). \tag{55}$$

In the nonrelativistic limit where $c \to \infty$, the negatively charged "−" components of the Klein-Gordon wave functions given in Eqs. (52) and (55), respectively, tend to the corresponding solutions of the nonrelativistic Schrödinger equation, while the "+" components vanish.

Making use of the Göppert-Meyer gauge transformation, we find that

$$H^{\text{KG}} = \frac{1}{2m}\Big[-i\hbar\nabla - \frac{e}{c}(\boldsymbol{r}\cdot\boldsymbol{\mathcal{E}})\hat{\boldsymbol{k}}_{\text{L}}\Big]^2 (i\sigma_y + \sigma_z) + mc^2\sigma_z + e\boldsymbol{r}\cdot\boldsymbol{\mathcal{E}} + V. \tag{56}$$

The Klein-Gordon SFA direct MPI amplitude is given by

$$\begin{aligned} T_{\boldsymbol{p},0}^{\text{KG}-\text{SFA}} &= \frac{1}{i\hbar}\int_{-\infty}^{\infty} dt \langle \bar{\chi}_{\boldsymbol{p}}(t)|H_{\text{Int}}^{\text{KG}}(t)\sigma_z|\bar{\phi}_0(t)\rangle \\ &= \frac{1}{i\hbar}\int_{-\infty}^{\infty} dt \langle \bar{\chi}_{\boldsymbol{p}}(t)|V\sigma_z|\bar{\phi}_0(t)\rangle. \end{aligned} \tag{57}$$

where in the second line of this equation we have, as above, integrated by parts. We now note that the positive charge component of the initial state, $\phi_0^+(\boldsymbol{r}, t)$, is a factor γ smaller than the negative charge component. We also observe that the final state positive charge component evaluated at the classical detachment time vanishes, that is, $\chi_{\boldsymbol{p}}^+(\boldsymbol{r}, t_d) = 0$, and at the saddle time $\chi_{\boldsymbol{p}}^+(\boldsymbol{r}, t_s)$ is a factor γ smaller than the corresponding final state negative charge component. Neglecting terms of order γ and higher in the transition amplitude therefore yields

$$\begin{aligned} T_{\boldsymbol{p},0}^{\text{KG-SFA}} = \frac{1}{i\hbar}\int_{-\infty}^{\infty} dt \left(\frac{E + 2mc^2 + \hbar\omega\beta(\omega t)}{2mc^2(1+\epsilon)^{1/2}(1+\gamma)^{1/2}}\right) \\ \times \langle \boldsymbol{\pi}(t)|V|\psi_0\rangle \exp[i\tilde{S}(t)], \end{aligned} \tag{58}$$

with $\epsilon = E/(mc^2)$, as above. The Coulomb matrix element is

$$\langle \boldsymbol{p}|V|\psi_0\rangle = C_\sigma \frac{1}{k} f[(\sigma - 1)/2, \kappa, k] \tag{59}$$

with

$$C_\sigma = -\frac{cZ\alpha(2\kappa)^{(\sigma+2)/2}}{(2\pi^2\hbar)^{1/2}\Gamma(\sigma+2)}. \tag{60}$$

Proceeding as before, we approximate the integral over time using the saddle point method and handle the resulting singularity in the Coulomb matrix element by setting $\sigma = 1$. We find that, making use of Eq. (45),

$$|T_{\boldsymbol{p},0}^{\text{KG}-\text{SFA}}|^2 = \frac{mc^2}{E + mc^2}|T_{\boldsymbol{p},0}^{\text{SFA}}|^2. \tag{61}$$

We have hereby obtained the result that, for light ions, the Klein-Gordon SFA transition probability is equal to the spin-unresolved Dirac SFA transition probability. This is consistent with the two-step interpretation of the ionization process. In the first step, the tunnel ionization of the electron is only weakly influenced by the electron spin, while the dynamics of the electron during the second step, namely the time-evolution of the "free" electron in the laser field, is essentially classical. We will return to this point below.

V. THE RELATIVISTIC SCHRÖDINGER EQUATION

We have seen that the negative energy components of the initial and final state Dirac wave functions give negligible contributions to the SFA direct ionization probability. Similarly, the positive charge components of the initial and final Klein-Gordon wave functions can also be neglected. This suggests that, to further simplify our treatment of the problem, we may use a manifestly single-particle relativistic theory. This can be accomplished by diagonalizing either the Dirac or Klein-Gordon Hamiltonian and then constructing approximate solutions of the resulting wave equations. An alternative approach, which we will consider here, is to make use of the relativistic Schrödinger equation (RSE) [7].

The RSE is not an obvious choice, and its shortcomings are well documented. In particular, the RSE cannot be expressed in a covariant form and it is "nonlocal" in the sense that the kinetic energy operator depends on all positive powers of the momentum operator. On the other hand, it is a single-particle theory and therefore the Born rule provides an interpretation of the RSE wave function.

Our starting point is the RSE describing a spinless particle in an electromagnetic field:

$$i\hbar\frac{\partial}{\partial t}\Psi(\boldsymbol{r}, t) = H^{\text{RS}}\Psi(\boldsymbol{r}, t), \tag{62}$$

where $H^{\text{RS}} = W + V$ and

$$W = [m^2c^4 + c^2(-i\hbar\nabla + e\boldsymbol{A})^2]^{1/2}. \tag{63}$$

The RSE satisfies the following second-order equation:

$$\left(i\hbar\frac{\partial}{\partial t} - V\right)^2\Psi(\boldsymbol{r}, t) = \left[W^2 + [W, V] + i\hbar\left(\frac{\partial W}{\partial t}\right)\right]\Psi(\boldsymbol{r}, t). \tag{64}$$

As a consequence, for the particular case in which the electron is moving only in the static potential $V(r)$ given by Eq. (5), the solution $\Psi(\boldsymbol{r}, t)$ of the RSE also satisfies the second-order equation

$$\left(i\hbar\frac{\partial}{\partial t} - V\right)^2\Psi(\boldsymbol{r}, t) = W_0^2\Psi(\boldsymbol{r}, t), \tag{65}$$

where

$$W_0 = [m^2c^4 + c^2(-i\hbar\nabla)^2]^{1/2}. \tag{66}$$

This is the Klein-Gordon equation for a particle moving in a Coulomb potential. The ground state wave function, $\psi_0(\boldsymbol{r})$, is given by Eq. (54).

Turning now to the situation in which $V = 0$, so that the particle interacts with only the laser pulse, Eq. (64) becomes

$$\left(i\hbar\frac{\partial}{\partial t}\right)^2\Psi(\boldsymbol{r}, t) = \left[W^2 + i\hbar\left(\frac{\partial W}{\partial t}\right)\right]\Psi(\boldsymbol{r}, t). \tag{67}$$

An approximate solution of this equation for a particle having momentum $\boldsymbol{p}$ is

$$\chi_{\boldsymbol{p}}^{\mathrm{RSV}}(\boldsymbol{r},t) = \left(\frac{E_p + \hbar\omega\beta(\eta)}{E_p}\right)^{1/2} \chi_{\boldsymbol{p}}(\boldsymbol{r},t). \quad (68)$$

It can be shown that these solutions are normalized to a Dirac delta function (for example, see the calculation of Boca in [38]), but are not orthogonal.

As usual, we will work in the Göppert-Mayer gauge, which yields

$$W = \left(m^2c^4 + c^2\left[-i\hbar\nabla - \frac{e}{c}(\boldsymbol{r}\cdot\boldsymbol{\mathcal{E}})\hat{\boldsymbol{k}}_{\mathrm{L}}\right]^2\right)^{1/2} + e\boldsymbol{r}\cdot\boldsymbol{\mathcal{E}}. \quad (69)$$

The RSE SFA direct MPI amplitude is given by

$$T_{\boldsymbol{p},0}^{\mathrm{RSE-SFA}} = \frac{1}{i\hbar}\int_{-\infty}^{\infty} dt \langle \chi_{\boldsymbol{p}}^{\mathrm{RSV}}(t) | H_{\mathrm{Int}}^{\mathrm{RS}}(t) | \phi_0(t)\rangle. \quad (70)$$

In this equation the initial state of the atomic system is $|\phi_0(t)\rangle = \exp[i(I_{\mathrm{p}} - mc^2)t/\hbar]|\psi_0\rangle$ and the interaction Hamiltonian can be written as

$$H_{\mathrm{Int}}^{\mathrm{RS}}(t) = W - (W_0 + V) + V. \quad (71)$$

Integrating Eq. (70) by parts leads to

$$\begin{aligned} T_{\boldsymbol{p},0}^{\mathrm{RSE-SFA}} &= \frac{1}{i\hbar}\int_{-\infty}^{\infty} dt \langle \chi_{\boldsymbol{p}}^{\mathrm{RSV}}(t) | V | \phi_0(t)\rangle \\ &= \frac{1}{i\hbar}\int_{-\infty}^{\infty} dt \left(\frac{E + mc^2 + \hbar\omega\beta(\omega t)}{E + mc^2}\right)^{1/2} \\ &\quad \times \langle \boldsymbol{\pi}(t)|V|\psi_0\rangle \exp[i\tilde{S}(t)]. \end{aligned} \quad (72)$$

Once again the integral over time is approximated using the saddle point method and the resulting singularity in the Coulomb matrix element is handled by setting $\sigma = 1$. Making use of Eq. (45), we find that

$$\left|T_{\boldsymbol{p},0}^{\mathrm{RSE-SFA}}\right|^2 = \frac{mc^2}{E + mc^2}\left|T_{\boldsymbol{p},0}^{\mathrm{SFA}}\right|^2, \quad (73)$$

which is in agreement, for light ions, with the results obtained using both the Dirac and Klein-Gordon equations.

VI. NUMERICAL EXAMPLE

In this section we present the results of numerical calculations of the SFA energy resolved direct MPI probability for hydrogenlike neon ions interacting with an ultrashort laser pulse. Let $U_{\mathrm{p}} = e^2\mathcal{E}_0^2/(4m\omega^2)$ be the electron ponderomotive energy. The ionization amplitude can then be parameterized in terms of four quantities. Firstly, the Keldysh parameter, $\gamma_K = [I_{\mathrm{p}}/(2U_{\mathrm{p}})]^{1/2}$, which is the ratio of the laser and tunneling frequencies and serves to help distinguish between the regimes where ionization can be understood as occurring via a tunneling process (γ_K comparable or less than unity) or by multiphoton ionization (γ_K larger than unity). Secondly, the scaled electric field strength $\bar{F} = me\mathcal{E}_0/(2mI_{\mathrm{p}})^{3/2}$ that, in the tunneling regime, must be small enough to preclude over-the-barrier ionization while being sufficiently large to allow ionization to occur with a significant probability. For the latter to be true, $\mathcal{E}_0$ must scale as Z^3. The nonrelativistic and relativistic regimes of the ejected electron dynamics can be demarcated via the scaled ponderomotive potential, $\bar{U} = U_{\mathrm{p}}/(mc^2)$. Finally, we have the scaled kinetic electron energy $\bar{E} = E/(2U_{\mathrm{p}})$ which, classically, is restricted to positive values less than or equal to unity.

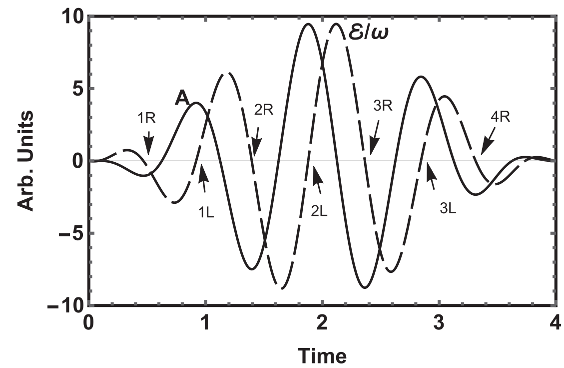

FIG. 1. The vector potential $\boldsymbol{A}(\omega t)$ (solid line) and the scaled electric field $\boldsymbol{\mathcal{E}}(\omega t)/\omega$ (dashed line) along the laser pulse polarization direction $\hat{\boldsymbol{\epsilon}}$, in arbitrary units, as a function of time, in units of the laser period, for the four-cycle pulse described in the text. The arrows point to particular moments during the pulse when the electric field is zero. The significance of these points in time is explained in the text.

For our example, we consider a four-cycle Ti:sapphire laser pulse of peak "instantaneous" intensity 3.00×10^{20} W/cm^2, which falls within the domain of currently achievable intensities of table-top Ti:sapphire laser systems. The laser pulse peak electric field and wavelength are, respectively, $\mathcal{E}_0 = 92.5$ a.u. (atomic units) and $\lambda = 800$ nm. For hydrogenlike neon, $\gamma = I_{\mathrm{p}}/(mc^2) = 2.66 \times 10^{-3}$ and $\bar{U} = 35.1$ so that the bound electron dynamics are essentially nonrelativistic while the ejected electron dynamics are typically relativistic. The scaled electric field strength is $\bar{F} = 9.25 \times 10^{-2}$ and the Keldysh parameter $\gamma_K = 6.16 \times 10^{-3}$, which implies that, at the peak of the pulse, ionization occurs deep in the tunneling regime. We also assume an ultrashort four-cycle pulse with duration $T = 8\pi/\omega$ and envelope function $\zeta(\eta) = \sin^2[\pi\eta/(\omega T)]$, and we set the pulse carrier-envelope phase to $\varphi = \pi/4$. In Fig. 1, $\boldsymbol{A}(\eta)$ as well as $\boldsymbol{\mathcal{E}}(\eta)/\omega$ are shown as a function of time along the laser polarization direction $\hat{\boldsymbol{\epsilon}}$.

Figures 2 and 3 illustrate how each of the saddle times contributes to the probability of the electron being ejected with a particular final energy along the parabola in the p_E-p_k plane described above. Referring to Eq. (37), every value of $|\boldsymbol{A}(\omega t)|$ during each of the half-cycles of the pulse gives rise to a saddle time contribution. As a consequence, there are two curves per half-cycle corresponding, respectively, to electron emission during the rise and fall of $|\boldsymbol{A}(\omega t)|$. During the half-cycle, the highest energy electrons are emitted as $|\boldsymbol{A}(\omega t)|$ reaches its local maximum (and $|\boldsymbol{\mathcal{E}}(\omega t)|$ passes through zero). At this point the two curves coalesce; the time during the laser pulse that these particular electrons are emitted is labeled in Fig. 1, the corresponding curves being labeled in

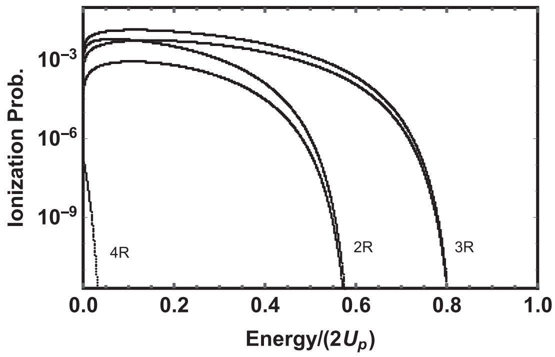

FIG. 2. The incoherent ionization probability corresponding to each saddle time that contributes to the emission probability of hydrogenlike neon at a given energy (in units of $2U_\mathrm{p}$) for electron emission at the angle of most probable emission (see text) in the right half of the $\hat{\boldsymbol{\epsilon}}$-$\hat{\boldsymbol{k}}_\mathrm{L}$ plane ($p_E > 0$). The laser pulse parameters are given in the text. The contributions corresponding to the highest electron energy per half-cycle, which are labeled 2R, 3R, and 4R, arise when the electric field of the laser pulse passes through zero (see Fig. 1). The contribution from 1R is negligible.

Figs. 2 and 3. Figure 2 corresponds to electron emission with the momentum component p_E along $\hat{\boldsymbol{\epsilon}}$ in the $\hat{\boldsymbol{\epsilon}}$-$\hat{\boldsymbol{k}}_\mathrm{L}$ plane, while for Fig. 3 emission is in the opposite half-plane. The calculations were carried out using Eq. (46). Referring to Figs. 1 and 3, the dominant contributions come from the half-cycle in which $|\boldsymbol{A}(\omega t)|$ is largest. In the ultrashort pulse regime, the saddle time contributions depend strongly on the choice of the pulse duration and the carrier-envelope phase φ [39]. However, typically the main contributions come from the saddle times that correspond to the cycle(s) when the pulse envelope is maximum. This is the case here, and is in agreement with the findings of Bauke *et al.* [28], who found that ionization in few-cycle intense laser pulses depends sensitively on the intensity at the peak of the pulse.

In Fig. 4 the angle integrated electron emission probability,

$$\frac{dP^{\mathrm{SFA}}(E)}{dE} = \left[\frac{m^2E(E+2mc^2)}{c^2}\right]^{1/2} \int \left|T^{\mathrm{SFA}}_{\boldsymbol{p},0}\right|^2 d\hat{\boldsymbol{p}}, \tag{74}$$

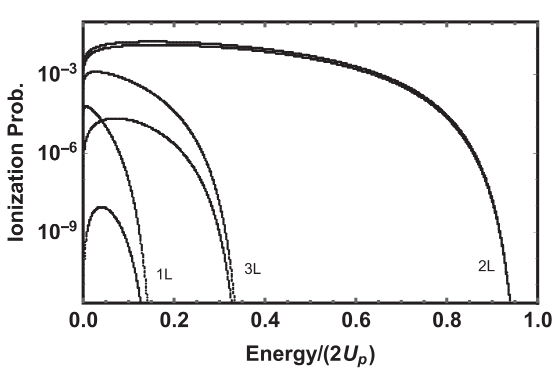

FIG. 3. The same as Fig. 2, but for electron emission in the left half of the $\hat{\boldsymbol{\epsilon}}$-$\hat{\boldsymbol{k}}_\mathrm{L}$ plane ($p_E < 0$). The contributions corresponding to the electrons emitted with the highest energy per half-cycle, which are labeled 1L, 2L, and 3L, arise when the electric field of the laser pulse passes through zero (see Fig. 1).

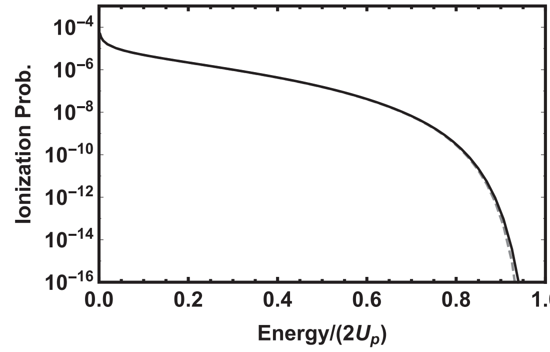

FIG. 4. The angle integrated energy resolved electron emission probability for the system discussed in the text. Also shown (gray dashed curve) is the same quantity obtained in the nonrelativistic theory. The curves are indistinguishable, aside from small differences near the classical cutoff energy.

is shown as a function of the electron energy, together with the results obtained using the nonrelativistic SFA. To obtain the results of Fig. 4 we have integrated over the incoherent sum of the saddle point contributions:

$$\left|T^{\mathrm{SFA}}_{\boldsymbol{p},0}\right|^2 d\hat{\boldsymbol{p}} \simeq \sum_{t_s} |a_{\mathrm{ion}}(t_s)|^2 d\hat{\boldsymbol{p}}. \tag{75}$$

The angle-integrated ionization probability is then a smooth function of E. Indeed, here we are interested in the main features of the electron energy distribution. These appear over energy scales that are much larger, of the order of mc^2, than the energy scales over which interference effects typically occur, namely, of the order of $\hbar\omega$. In particular, the width of the distribution of the ejected electrons in the $\hat{\boldsymbol{\epsilon}}$-$\hat{\boldsymbol{k}}_\mathrm{L}$ plane and about the most likely polar emission angle θ^{m}, where $\sin\theta^{\mathrm{m}} \simeq [2mc^2/(E+2mc^2)]^{1/2}$, scales approximately as $(\bar{F}\gamma_K^2)^{1/2}$. We recall that interferences are governed by the phases between saddle contributions with ionization amplitudes having comparable magnitudes. The rate at which these phases vary as a function of the polar angle θ is much greater than $(\bar{F}\gamma_K^2)^{1/2}$. Therefore, the phases vary rapidly with respect to changes in the emission angles that are small relative to the width of the angular distribution. This has the consequence that the MPI process of an ion in the (ultrashort) laser pulse can be understood in terms of the well-known adiabatic semiclassical model [7]. In this model, the electron is first ejected by a tunneling mechanism with probability proportional to $|a_{\mathrm{ion}}|^2$, thereby emerging with near zero momentum in the laser field. The electron is subsequently treated as a classical particle that interacts with the laser field, whereby it acquires its final momentum $\boldsymbol{p}$.

In Fig. 4, the angle-integrated ionization probability calculated using the nonrelativistic SFA MPI formula is also shown. With the exception of the small differences at high electron energies, the agreement between the relativistic and nonrelativistic results is good. In order to understand why the relativistic and nonrelativistic results are in close agreement, let us evaluate the SFA direct MPI probability density about the most probable angle of emission, where $\Lambda \simeq 1 - \gamma/3 \simeq 1$ and $\theta \simeq \theta^{\mathrm{m}}$. Using the approximation of Equation (75) and defining

$\delta\theta = \theta - \theta^{\rm m}$ and $\delta p_k = p_k - p_k^{\rm m} \simeq -p\sin\theta^{\rm m}\sin(\delta\theta)$ as the difference between p_k and its most likely value, we see that

$$dP^{\rm SFA}(E,\hat{\boldsymbol p}) \simeq (2m^3E)^{1/2}dE\,d(\delta\theta)d\phi \sum_{t_s} \frac{(c\alpha Z)^2\hbar\kappa^3}{4I_{\rm p}|e\mathcal{E}(\omega t_d)|^2} \times \exp\left(-\frac{2[(\delta p_k)^2 + p_B^2 + 2mI_{\rm p}]^{3/2}}{3m|e\mathcal{E}(\omega t_d)|}\right), \quad (76)$$

where $p_B = p\sin(\theta^{\rm m} + \delta\theta)\sin\phi$. This expression is of exactly the same form as the corresponding nonrelativistic formula [7]. However, in the nonrelativistic limit emission is most probable along $\pm\hat{\boldsymbol\epsilon}$ ($\theta^{\rm m} = \pi/2$, $\phi = 0, \pi$) so that $\delta p_k = -p\sin(\delta\theta)$ and $p_B = p\cos(\delta\theta)\sin\phi$. It would be of interest to extend Eq. (76) to include heavier ions by including high-order corrections involving the parameter γ.

VII. CONCLUSION

We have investigated the MPI of light hydrogenlike ions by ultrashort, infrared laser pulses with peak intensities that are sufficiently high that relativistic effects are important. We have shown that the spin-unresolved differential SFA MPI probability obtained using the Dirac equation agrees with both the Klein-Gordon and RSE differential MPI probabilities. Moreover, deep in the tunneling regime, the angle-integrated SFA MPI probabilities are given by the corresponding nonrelativistic formula, properly adjusted to account for the momentum component of the electron in the laser pulse propagation direction. This provides a very simple framework for analyzing the angle-integrated electron energy spectrum of ions interacting with short, intense infrared laser pulses well into the relativistic regime. Our work also indicates that, for spin-unresolved investigations of intense-laser atom interactions, the Klein-Gordon equation could be used as a simpler alternative to the Dirac equation.

[1] S. Bahk *et al.*, Opt. Lett. **29**, 2837 (2004).
[2] W. Yan *et al.*, Nat. Photonics **11**, 514 (2017).
[3] L. V. Keldysh, Sov. Phys. JETP **20**, 1307 (1965).
[4] F. H. M. Faisal, J. Phys. B **6**, L89 (1973).
[5] H. R. Reiss, Phys. Rev. A **22**, 1786 (1980).
[6] M. Lewenstein and A. L'Huillier, in *Strong Field Laser Physics*, Springer Series in Optical Sciences Vol. 134 (Springer, New York, 2009), p. 147.
[7] C. J. Joachain, N. J. Kylstra, and R. M. Potvliege, *Atoms in Intense Laser Fields* (Cambridge University Press, Cambridge, 2012).
[8] P. Salières, in *Atoms, Solids and Plasmas in Super-Intense Laser Fields*, edited by D. Batani, C. J. Joachain, S. Martellucci, and A. N. Chester (Kluwer, New York, 2001), p. 83.
[9] M. Lewenstein, P. Balcou, M. Y. Ivanov, A. L'Huillier, and P. B. Corkum, Phys. Rev. A **49**, 2117 (1994).
[10] P. Salières, P. Antoine, A. de Bohan, and M. Lewenstein, Phys. Rev. Lett. **81**, 5544 (1998).
[11] G. Paulus, W. Becker, W. Nicklich, and H. Walther, J. Phys. B **27**, L703 (1994).
[12] A. Becker and F. H. M. Faisal, J. Phys. B **29**, L197 (1996).
[13] N. Suárez, A. Chacón, M. F. Ciappina, J. Biegert, and M. Lewenstein, Phys. Rev. A **92**, 063421 (2015).
[14] T. Keil, S. V. Popruzhenko, and D. Bauer, Phys. Rev. Lett. **117**, 243003 (2016).
[15] F. H. M. Faisal, Phys. Rev. A **94**, 031401(R) (2016).
[16] M. Klaiber, J. Daněk, E. Yakaboylu, K. Z. Hatsagortsyan, and C. H. Keitel, Phys. Rev. A **95**, 023403 (2017).
[17] H. R. Reiss, Phys. Rev. A **42**, 1476 (1990).
[18] M. Klaiber, K. Z. Hatsagortsyan, and C. H. Keitel, Phys. Rev. A **74**, 051803(R) (2006).
[19] M. Klaiber, K. Z. Hatsagortsyan, and C. H. Keitel, Phys. Rev. Lett. **114**, 083001 (2015).
[20] M. Klaiber, K. Z. Hatsagortsyan, J. Wu, S. S. Luo, P. Grugan, and B. C. Walker, Phys. Rev. Lett. **118**, 093001 (2017).
[21] N. Milosevic, V. P. Krainov, and T. Brabec, J. Phys. B: At., Mol. Opt. Phys. **35**, 3515 (2002).
[22] M. Klaiber, E. Yakaboylu, H. Bauke, K. Z. Hatsagortsyan, and C. H. Keitel, Phys. Rev. Lett. **110**, 153004 (2013).
[23] E. Yakaboylu, M. Klaiber, H. Bauke, K. Z. Hatsagortsyan, and C. H. Keitel, Phys. Rev. A **88**, 063421 (2013).
[24] M. Klaiber, E. Yakaboylu, and K. Z. Hatsagortsyan, Phys. Rev. A **87**, 023418 (2013).
[25] M. Klaiber *et al.*, J. Phys. B: At., Mol. Opt. Phys. **47**, 065603 (2014).
[26] E. Yakaboylu, M. Klaiber, and K. Z. Hatsagortsyan, Phys. Rev. A **91**, 063407 (2015).
[27] K. Krajewska and J. Z. Kamiński, Phys. Rev. A **94**, 013402 (2016).
[28] H. Bauke, H. G. Hetzheim, G. R. Mocken, M. Ruf, and C. H. Keitel, Phys. Rev. A **83**, 063414 (2011).
[29] S. Selstø, E. Lindroth, and J. Bengtsson, Phys. Rev. A **79**, 043418 (2009).
[30] Y. V. Vanne and A. Saenz, Phys. Rev. A **85**, 033411 (2012).
[31] A. S. Simonsen, T. Kjellsson, M. Førre, E. Lindroth, and S. Selstø, Phys. Rev. A **93**, 053411 (2016).
[32] I. V. Ivanova, V. M. Shabaev, D. A. Telnov, and A. Saenz, Phys. Rev. A **98**, 063402 (2018).
[33] J. D. Bjorken and S. D. Drell, *Relativistic Quantum Mechanics* (McGraw-Hill, New York, 1964).
[34] D. M. Volkov, Z. Phys. **94**, 250 (1935).
[35] M. Y. Ivanov, T. Brabec, and N. Burnett, Phys. Rev. A **54**, 742 (1996).
[36] H. Feshbach and F. Villars, Rev. Mod. Phys. **30**, 24 (1958).
[37] L. I. Schiff, *Quantum Mechanics* (McGraw-Hill, New York, 1955).
[38] M. Boca, J. Phys. A **44**, 445303 (2011).
[39] R. M. Potvliege, N. J. Kylstra, and C. J. Joachain, J. Phys. B **33**, L743 (2000).